



Regulatory role of sorting nexin 5 in protein stability and vesicular targeting of vesicular acetylcholine transporter to synaptic vesicle-like vesicles in PC12 cells

Meihen Sun^{1,Δ}, Xu Han^{1,Δ}, Fei Chang^{2,Δ}, Hongfei Xu³, Lesley Colgan^{4,✉}, Yongjian Liu^{1,✉}

¹Jiangsu Key Laboratory of Xenotransplantation, and Department of Medical Genetics, Nanjing Medical University, Nanjing, Jiangsu 211166, China;

²Neuroscience Program, University of Utah School of Medicine, Salt Lake City, UT 84112, USA;

³Department of Neurology, University of California San Francisco School of Medicine, San Francisco, CA 94143, USA;

⁴Max Planck Florida Institute for Neuroscience, Jupiter, FL 33458, USA.

Abstract

Accurate targeting of vesicular acetylcholine transporter (VACHT) to synaptic vesicles (SVs) is indispensable for efficient cholinergic transmission. Previous studies have suggested that the dileucine motif within the C-terminus of the transporter is sufficient for its targeting to SVs. However, the cytosolic machinery underlying specific regulation of VACHT trafficking and targeting to SVs is still unclear. Here we used the C-terminus of VACHT as a bait in a yeast two-hybrid screen to identify sorting nexin 5 (SNX5) as its novel interacting protein. SNX5 was detected in the SVs enriched LP2 subcellular fraction of rat brain homogenate and showed strong colocalization with VACHT in both brain sections and PC12 cells. Binding assays suggested that the C-terminal domain of VACHT can interact with both BAR and PX domain of SNX5. Depletion of SNX5 enhanced the degradation of VACHT and the process was mediated through the lysosomal pathway. More importantly, we found that, in PC12 cells, the depletion of SNX5 expression significantly decreased the synaptic vesicle-like vesicles (SVLVs) localization of VACHT. Therefore, the results suggest that SNX5 is a novel regulator for both stability and SV targeting of VACHT.

Keywords: retrograde trafficking, vesicular targeting, synaptic vesicle-like vesicles, synaptic vesicles, PC12

Introduction

Efficient and precise packaging of classical neurotransmitters into synaptic vesicles (SVs) at the nerve terminals is secured by a specific group of

vesicular transport proteins such as vesicular acetylcholine transporters (VACHTs)^[1]. Increasing evidence has indicated that the vesicular targeting and expression of vesicular transport proteins can strongly influence the amount of neurotransmitters packaged

^ΔThese authors contributed equally to this work.

[✉]Corresponding authors: Yongjian Liu, Jiangsu Key Laboratory of Xenotransplantation, and Department of Medical Genetics, Nanjing Medical University, Nanjing, Jiangsu 211166, China. Tel: +86-25-86869442, E-mail: young.liu78@gmail.com; Lesley Colgan, Max Planck Florida Institute for Neuroscience, Jupiter, FL 33458, USA. Tel: +1-561-972-9210, E-mail: lesley.colgan@nufi.org.

Received: 17 June 2020; Revised: 19 June 2020; Accepted: 19

© 2021 by the Journal of Biomedical Research.

June 2020; Published online: 21 August 2020

CLC number: Q7, Document code: A

The authors reported no conflict of interests.

This is an open access article under the Creative Commons Attribution (CC BY 4.0) license, which permits others to distribute, remix, adapt and build upon this work, for commercial use, provided the original work is properly cited.

into the secretory vesicles as well as quantal size^[2]. Thus, the molecular mechanisms underlying recycling and vesicular targeting of these transport proteins would provide important insight in the regulated synaptic transmission and pathogenesis of neurological diseases such as Parkinson disease^[3]. Interestingly, membrane targeting of VACHT to SVs has been shown to be regulated by the trafficking signals in its C-terminus^[4-6]. Specifically, we have showed that a dileucine motif within its C-terminal domain is required for its endocytosis and sufficient for SV sorting^[5]. Additionally, a serine residue upstream of the dileucine motif undergoes regulated phosphorylation which can drive a portion of VACHT into the secretory pathway and away from large dense core vesicles (LDCVs) in PC12 cells^[6]. Furthermore, similar to VACHT, another vesicular transport protein, vesicular glutamate transporter 1 (VGLUT1) also utilizes a dileucine-like motif in its C-terminus for its targeting to SVs^[7]. However, the cytosolic machinery responsible for regulating such dileucine-based SV targeting motifs remains elusive.

It is well known that trafficking and targeting of functional SV membrane proteins are highly regulated through vesicular formation and cytosolic machinery mediated molecular events^[8]. Constitutively targeted SV proteins at the synaptic terminal membrane undergo *en route* exo-endocytosis processes to functional SVs in presumably readily releasable pool^[9-12]. Equally important is that how molecular regulators are required for governing their precise recruitment either directly at the endocytic process or later at the endosomal sorting. One of such cytosolic proteins determining the endocytosis of SV protein VACHT at the plasma membrane was reported to be adaptor protein 2 (AP2), largely through its interaction with the dileucine motif and a non-classical tyrosine-containing motif in the C-terminal domain of VACHT^[6,13-14]. However, either the dileucine motif itself or its interaction with AP2 may not explain the further SV targeting steps after internalization. As an alternative pathway for SV biogenesis through AP3 mediated mechanism, the interaction of this adaptor protein with the di-hydrophobic Met-Leu motif in the C-terminus of synaptotagmin-1 seems to be responsible for sorting the SV protein from endosome to SVs^[15]. VGLUT1 relies on the interaction of its C-terminal polyproline domains with endophilins to target to glutamatergic synaptic vesicles^[16-17]. Thus, the vesicular sorting of SV proteins is believed to mainly depend on the interaction of their C-terminal domains with cytosolic proteins, while the specific cytosolic machinery that targets VACHT to SVs

remains unidentified.

To investigate such cytosolic machinery specifically for targeting VACHT to SVs, we performed a yeast two-hybrid (Y2H) screen using the C-terminal domain of VACHT as bait and found a novel interacting protein sorting nexin 5 (SNX5). SNX5 was identified as binding partner of SNX1 and thus defined as the Vps17p homolog of mammalian cells for the retromer complex^[18]. As an important member of the sorting nexin family, it is characterized by its phospholipid-binding phox (PX) domain and a membrane-curvature-sensing and membrane-binding Bin-Amphiphysin-Rvs (BAR) domain^[19]. Interestingly, its PX domain can uniquely bind to PI(4,5)P₂, different from other SNXs which mainly bind to PI3-phosphate (PI3P)^[20]. More importantly, SNX5 was identified as a key membrane associated protein in the purified SVs from rat brain by mass spectrometry^[21], strongly indicating its role in regulating SV function.

In the present report, we identified SNX5 as a novel and specific binding partner for VACHT. Through its interaction with the C-terminal domain of VACHT, SNX5 regulates the stability of VACHT, away from degradation by lysosomal pathway. We have shown that depleted SNX5 expression in HeLa cells led to decreased half-life of VACHT. Deletion of SNX5 in PC12 cells resulted in VACHT mistargeting to LDCVs, suggesting that SNX5 may facilitate the SV targeting of VACHT in PC12 cells. Therefore, our data indicated that SNX5 is essential in regulating the trafficking of VACHT.

Materials and methods

Animals

Adult Sprague-Dawley (SD) rats (200–250 g) were purchased from Animal Core Facility of Nanjing Medical University. All rats were maintained at a controlled temperature ([20±2] °C) and group housed (12-hour light/dark cycle) with access to food and water *ad libitum*. All procedures involving the use of animals were approved by the Institution Animal Care and Use committee of Nanjing Medical University. Every effort was made to minimize the number of animals used and their suffering.

Chemicals and antibodies

Following reagents were purchased from Sigma Chemical Co. (USA): cycloheximide (CHX), leupeptin, ammonium chloride (NH₄Cl), G418 and nerve growth factor (NGF). Matrigel was purchased

from Becton Dickinson (USA). Following reagents were purchased from Thermo Fisher (USA): protein A/G agarose, Dulbecco's Modified Eagle Medium (DMEM), Lipofectamine 2000, and penicillin/streptomycin. Cosmic calf serum (CCS), donor equine serum (DES), and fetal bovine serum (FBS) were from HyClone (GE Healthcare Life Science, USA). All the restriction enzymes and products related to plasmid constructions were from NEB (USA). The following primary antibodies were used: mouse monoclonal anti-HA (Covance, USA), rabbit polyclonal anti-HA (Covance), mouse monoclonal anti-Flag (Sigma), rabbit polyclonal anti-Flag (Sigma), rabbit polyclonal anti-IL-2R alpha and goat polyclonal anti-SNX5 (Santa Cruz Biotech., USA), mouse monoclonal anti-synaptophysin and rabbit polyclonal anti-secretogranin II (Sg II) (Synaptic Systems, Germany), mouse monoclonal anti-LAMP1 (Thermo Fisher), mouse monoclonal anti-actin and anti-GAPDH (Sigma). The following secondary antibodies from Thermo Fisher were used: Alexa 488-conjugated donkey anti-mouse secondary antibody, Alexa 488-conjugated donkey anti-rabbit secondary antibody, Alex 488-conjugated donkey anti-goat secondary antibody, Alexa568-conjugated donkey anti-mouse secondary antibody, Alexa 568-conjugated donkey anti-mouse secondary antibody, HRP-conjugated goat anti-mouse secondary antibody, HRP-conjugated goat anti-rabbit secondary antibody, and HRP-conjugated rabbit anti-goat secondary antibody.

Plasmid construction and mutagenesis

The following constructs were used in this study: pcDNA3.1-TacA, pcDNA3.1-3HA/Flag-VACHT, pcDNA3.1-3HA/Flag-SNX5, pET15b-SNX5, pET15b-SNX5-PX, and pET15b-SNX5-BAR. The pcDNA3.1-TacA plasmid was constructed following a previously described protocol^[5]. Briefly, the full-length of rat VACHT (GeneBank accession no. U09838) was amplified by PCR and then inserted into pcDNA3.1-3HA/Flag vector. The full-length of SNX5 and two deletion mutants (SNX5-PX and SNX5-BAR) were amplified by PCR and then inserted into pET15b for pull down assays.

Cell culture and transfection

All cells were maintained in 5% CO₂ at 37 °C in medium containing penicillin and streptomycin unless otherwise noted. HeLa Swiss and COS7 cells were maintained in DMEM supplemented with 10% CCS and 1% penicillin/streptomycin, while PC12 cells were maintained in DMEM with 10% horse serum, 5% FBS and 1% penicillin/streptomycin.

Stable lines of TacA were generated by further selection with G418 (500 mg/mL). Positive transformants were screened by immunofluorescence staining and Western blotting analysis. At least, the stable lines were tested for consistent subcellular localization of the heterogeneously expressed membrane proteins.

Tissue preparation

Tissues were dissected from adult rats and homogenized with a Teflon pestle in lysis buffer (150 mmol/L NaCl, 50 mmol/L Tris-HCl, pH 8.0, 5 mmol/L EDTA and 1% NP-40 containing protease inhibitors).

Preparation of synaptic vesicles from rat brain

Synaptic vesicles were prepared as described previously^[22]. Rat brains were removed and homogenized in homogenization buffer (320 mmol/L sucrose, 4 mmol/L HEPES-NaOH, pH 7.3 containing protease inhibitor) on ice. The homogenates (H) were centrifuged for 10 minutes at 1000 g to separate the supernatant (S1) from the nuclei and large debris fraction. The S1 fraction was centrifuged at 12 000 g for 15 minutes to separate the supernatant (S2, small cell fragment) and the pellet (P2). The P2 fraction was resuspended in 10 mL homogenization buffer and centrifuged at 13 000 g for 15 minutes. The pellet (P2') was collected and resuspended in homogenization buffer to get the synaptosomal fraction. P2' pellet was resuspended and centrifuged at 25 000 g for 20 minutes at 4 °C to get LP1 (synaptic membranes) and LS1 (synaptosome cytosol and synaptic vesicles). LS1 was centrifuged at 165 000 g for 2 hours at 4 °C to get LP2 (synaptic vesicles) and LS2 (synaptic cytosol).

Immunofluorescence and confocal microscopy

For tissue staining: adult SD rats ($n=4$) were anesthetized with 4% chloral hydrate, and transcardially perfused with 0.9% saline followed by 4% paraformaldehyde (PFA) for fixation. Brains were removed and cryoprotected in 30% sucrose at 4 °C. Sections (50- μ m thick) were cut using a freezing-sliding microtome and collected in 10 mmol/L PBS, pH 7.4. After blocked in PBS with 0.3% Triton X-100 and 1% BSA for 30 minutes, sections were incubated with primary antibody at 4 °C overnight and followed by the appropriate Alexa conjugated secondary antibody.

For cell staining: the process was performed as previously described^[23]. In brief, cells seeded on coverslips were transfected using Lipofectamin 2000 according to the manufacturer's instructions. Twenty-four hours later, cells were fixed with 4% PFA

followed by permeabilized and blocking for 30 minutes in blocking solution (2% BSA, 1% fish skin gelatin, and 0.02% saponin in PBS). Cells were then incubated with primary antibody in blocking solution for 1 hour at room temperature and followed by incubation with the appropriate Alexa 488 or 588-conjugated secondary antibody for 1 hour.

For confocal laser microscopy, staining was visualized with a confocal laser microscope (Carl Zeiss, LSM 710, Germany) and the images processed using the NIH ImageJ program and ZEN program.

Co-immunoprecipitation

To analyze protein interaction *in vitro*, COS7 cells transfected with different expression constructs were lysed in NP-40 lysis buffer (150 mmol/L NaCl, 50 mmol/L Tris-HCl, pH 8.0, 5 mmol/L EDTA, and 0.5% NP-40 containing protease inhibitors) for 10 minutes on ice. Cell lysate was centrifuged at 1600 g and the supernatants were then precleared by incubation for 60 minutes at 4 °C with 30 µL protein A/G agarose beads and centrifugation at 8000 g for 5 minutes. The precleared lysates were incubated for 2 hours at 4 °C with 30 µL protein A/G agarose beads bound to polyclonal antibody to tagged protein. After immunoprecipitation, the beads were washed in wash buffer (0.5% NP-40, 150 mmol/L NaCl, 50 mmol/L Tris-HCl, pH 7.0, and 5 mmol/L EDTA) and then processed for SDS-PAGE analysis.

Pull-down assay

GST or His-tagged fusion recombinant proteins were produced in *Escherichia coli* BL21 cells using 0.1 mmol/L isopropyl-beta-D-thiogalactopyranoside for induction at room temperature for 4 to 6 hours. The recovered bacteria were lysed with sonication in lysis buffer (PBS with 0.2% [w/v] Triton X-100; and protease inhibitors). Fusion protein was purified with GST agarose or with Ni-NTA agarose (for His fusion protein). The recombinant proteins were detected by coomassie brilliant blue. COS7 cells transfected with different expression constructs were lysed in NP-40 buffer (150 mmol/L NaCl, 50 mmol/L Tris-HCl, pH 8.0, 5 mmol/L EDTA and 0.5% NP-40 containing protease inhibitors). Lysates were incubated with recombinant proteins for 60 minutes at 4 °C. After centrifugation at 20 000 g for 15 minutes, the supernatants were transferred to new Eppendorf tubes and the pellets were resuspended in 1× SDS-sample buffer. Aliquots corresponding to 1/25 of each supernatant and 1/4 of each pellet were analyzed by SDS-PAGE.

Sucrose gradient and fractionation analysis

Sucrose gradients were prepared using a gradient

mixer to form continuous gradients with sucrose concentrations from 0.65 mol/L to 1.55 mol/L. PC12 cells stably expressing TacA were harvested in Buffer A (150 mmol/L NaCl, 10 mmol/L HEPES pH 7.4, 1 mmol/L EGTA, and 0.1 mmol/L MgCl₂) with protease inhibitors. Cells were cracked by eight passes through a cell cracker (clearance: 0.02 mm). Postnuclear supernatants were then loaded onto prepared density or velocity gradients and spun in a Beckman SW41 rotor at 30 000 g for 6 hours at 4 °C (Beckman Instruments, USA). Fractions from density gradients were collected from the top and all gradients were numbered from light to heavy.

VACHT half-life assays

HeLa cells were transfected with different expression constructs using Lipofactamin 2000 in 12-well plates and incubated for 72 hours, and CHX at 100 µg/mL was added to the cells for the indicated time points. Cells were lysed and subjected to Western blotting analysis.

Pharmacological treatments of cycloheximide and lysosomal inhibitors

Cells were incubated for 8 hours with CHX (100 µg/mL), with or without presence of 100 µg/mL leupeptin and 50 mmol/L NH₄Cl. After treatment, cells were lysed and subjected to Western blotting analysis.

Western blotting analysis

Proteins in sample buffer were separated by electrophoresis through discontinuous 10% SDS-polyacrylamide gels before electrotransfer to nitrocellulose membrane (Merck Millipore, USA). The filters were then blocked in TBS containing 0.1% Tween-20 (TBST) and 5% nonfat dry milk, incubated in TBST with 1% nonfat dry milk and primary antibody at dilutions ranged from 1:1000 to 1:10 000, washed in TBST, and incubated in appropriate secondary antibody conjugated to peroxidase followed by washing in TBST and visualization by enhanced chemiluminescence with the Tanon 5200 gel imaging system (Tanon, China).

Statistical analysis

Graphing and statistics were performed using Origin 8.0. Unpaired, two-tailed *t*-tests, and one-way ANOVA were used to calculate *P*-values for all bar graph analyses.

Results

Association of SNX5 with VACHT in brain tissues

To investigate the cytosolic mechanism that

presumably regulates the vesicular targeting of VACHT, we performed a Y2H screening to identify the potential interacting proteins for VACHT. We used the C-terminus of VACHT as bait and identified SNX5 as a novel binding protein (data not shown). Given the results of a mass spectrometry study showing that SNX5 was identified as a membrane-associated protein in SVs^[21], we firstly characterized the tissue distribution of SNX5 in the nerve system. Using Western blotting analysis with a commercial antibody, we found that the protein expression of SNX5 was

displayed relatively widespread tissue distribution pattern. As shown in **Fig. 1A**, the high levels of SNX5 protein were found in the brain, lung, liver, testis, and kidney. Furthermore, to test whether SNX5 specifically expressed on SVs, we performed differential centrifugation to purify SVs from rat brains. Consistent with the previous proteomic results, SNX5 was found in the SV enriched LP2 subcellular fraction of rat brain homogenate (**Fig. 1B**). To determine whether the endogenous distribution of SNX5 is associated with the SVs, we performed the

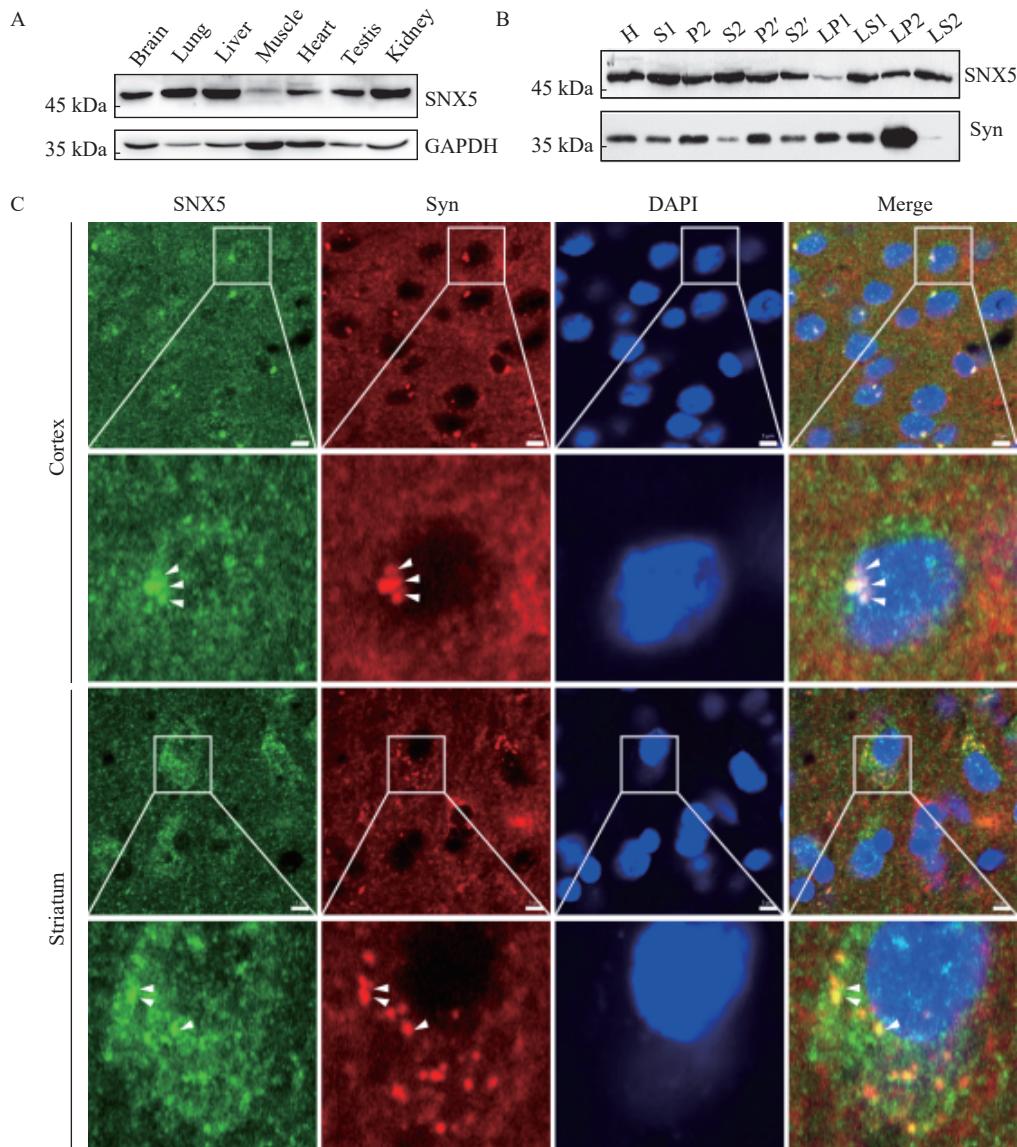


Fig. 1 SNX5 was enriched in rat brain and associated with synaptic vesicles. A: SNX5 expression at protein levels in different tissues was analyzed by Western blotting. Proteins from multiple tissues were blotted with SNX5 polyclonal antibody. Protein sample loading was normalized with protein total concentration. GAPDH expression was used as an internal control. B: Subcellular localization of SNX5 was analyzed by Western blotting using a series of fractions from rat brains upon differential centrifugation. Synaptophysin (Syn) was used as the marker of synaptic vesicles. C: Co-localization between SNX5 and synaptophysin was tested in rat brain regions by immunohistochemistry. In both cortex (upper panel) and striatum (lower panel), SNX5 (green) was mainly present in cell bodies and partially in fibers while synaptophysin (red), the marker of synaptic vesicles, was present in both neurons and fibers. SNX5-positive puncta was significantly co-localized with synaptophysin in cell bodies (yellow puncta, indicated by white arrow head). Scale bar, 5 μ m.

immunohistochemistry to examine the co-localization of SNX5 and SV marker protein synaptophysin in different brain regions. As shown in **Fig. 1C**, microscopic images of brain sections revealed that SNX5 was widespread in brain regions, including the cortex, striatum, and hippocampus. More importantly, punctate stainings of SNX5 in neurons were significantly co-localized with synaptophysin in these regions. Taken together, these results indicated that SNX5 was enriched in the brain and specifically associated with SVs, further suggesting a potential role of SNX5 in regulating function and trafficking of SV membrane proteins such as VACHT.

VACHT specifically interacts with SNX5

To confirm the interaction between SNX5 and VACHT resulted from Y2H screening, we performed the co-immunoprecipitation (Co-IP) assay. HA-tagged

VACHT and Flag-tagged SNX5 were co-transfected into COS7 cells and the Co-IP result showed that VACHT could pull down SNX5 (**Fig. 2A**). Moreover, to confirm endogenous interaction between SNX5 and VACHT, we used rat synaptosome lysates to perform Co-IP and found that endogenous VACHT interacted specifically with SNX5 (**Fig. 2B**). Additionally, immunofluorescent staining was used to test the colocalization between SNX5 and VACHT. In PC12 cells, SNX5 was found to partially colocalize with synaptophysin, further confirming the specific distribution of SNX5 in SVs (**Fig. 2C**). Both the results of the Y2H and our previous work have revealed that the C-terminus of VACHT sufficiently mediated its SV targeting through a dileucine motif⁵¹. Here we used TacA, a chimeric protein fused VACHT C-terminus with an unrelated protein, Tac, to mimic the function of C-terminus of VACHT. Double

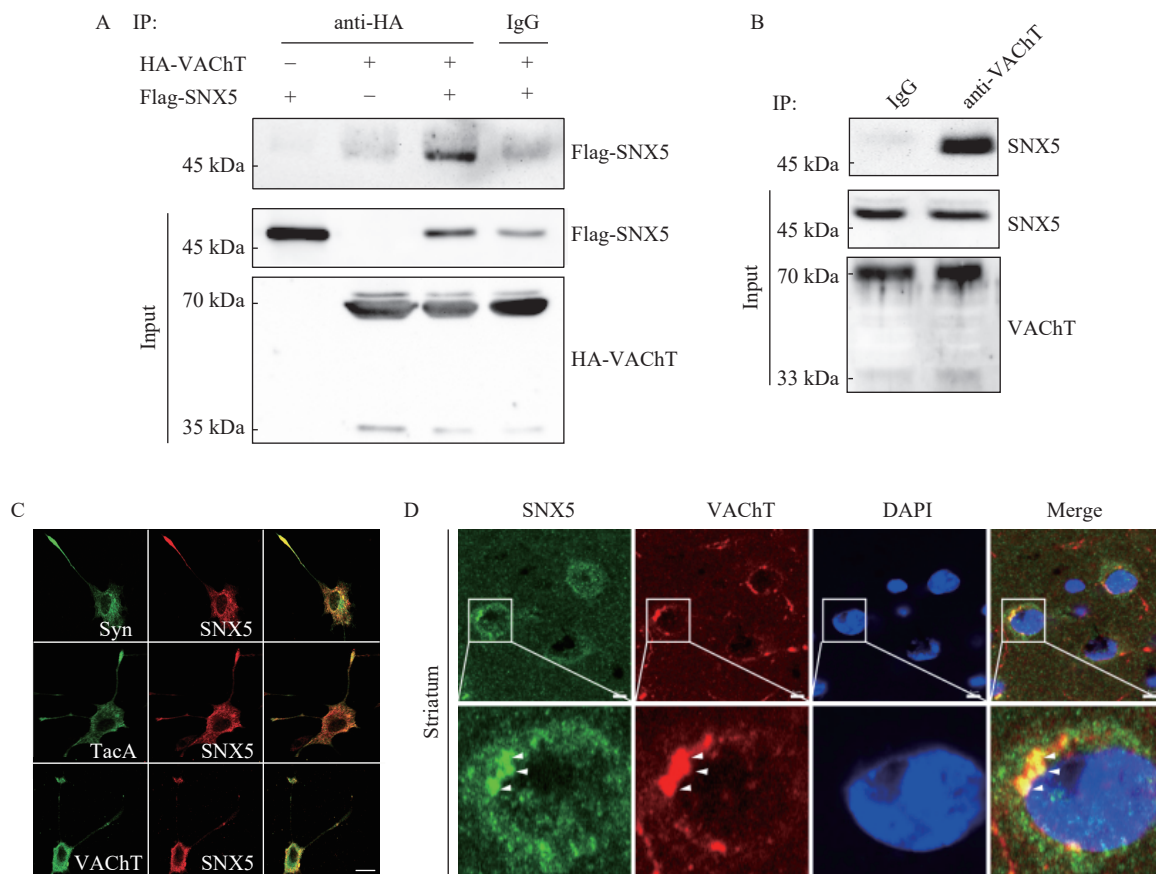


Fig. 2 VACHT specifically interacted with SNX5. A: Both HA-VACHT and Flag-SNX5 were transiently overexpressed in COS7 cells, followed by cell lysates immunoprecipitated with anti-HA antibody and then analyzed with anti-Flag antibody using Western blotting. B: Interaction of endogenous SNX5 with VACHT was analyzed in rat brain synaptosomes. Cell lysates were immunoprecipitated with anti-VACHT antibody and detected with anti-SNX5 antibody by Western blotting. C: Co-localization of SNX5 with synaptophysin (upper panel), TacA (middle panel) and VACHT (lower panel) was tested by immunofluorescent staining in differentiated PC12 cells. SNX5, synaptophysin, TacA, and VACHT were detected with specific antibodies. Scale bar, 10 μ m. D: Co-localization between SNX5 and VACHT was tested in rat striatum by immunohistochemistry. In striatum, SNX5 (Green) was mainly present in cell bodies and rarely in fibers while VACHT (red) was present in both neurons and fibers. SNX5-positive puncta was significantly co-localized with VACHT in a perinuclear pattern (yellow puncta, indicated by white arrow head). Scale bar, 5 μ m.

immunofluorescence staining and confocal microscopy of PC12 cells revealed that SNX5 significantly co-localized with TacA and VACHT (**Fig. 2C**). We also tested the co-localization between SNX5 and VACHT in the rat brains using immunohistochemistry. Our results showed that VACHT-immunoreactive fibers were present in many brain regions, such as the cortex, hippocampus, and striatum (data not shown), while VACHT positive neurons were present in the striatum (**Fig. 2D**), which is consistent with previous reports^[24]. Furthermore, SNX5 and VACHT were considerably co-localized (**Fig. 2D**). These findings suggested that SNX5 could specifically interact with VACHT.

To consolidate this conclusion, we performed recombinant binding assay. The result of pull-down assays showed that GST-tagged SNX5 directly interacted with VACHT (**Fig. 3B**). Using TacA to perform GST pull-down assay, we confirmed that the interaction between SNX5 and VACHT is mediated by

the C-terminus of VACHT (**Fig. 3C**). Since SNX5 is composed of a PX domain and a BAR domain, we next investigated which domain determines its interaction with VACHT. The recombinant binding assays showed that both PX domain and BAR domain could interact with TacA (**Fig. 3D**). Collectively, these data demonstrated that VACHT interacts with both PX and BAR domain of SNX5 through its C-terminus.

Depleted SNX5 expression induced the instability of VACHT

SNX5 has been suggested to regulate membrane proteins trafficking from endosome to trans-Golgi network (TGN), presumably preventing them from lysosomal degradation. To determine whether SNX5 could affect the stability of VACHT, we performed CHX chase assays in HeLa cells overexpressing VACHT. The expression level of VACHT was stable over the course of 9 hours in control cells. In contrast,

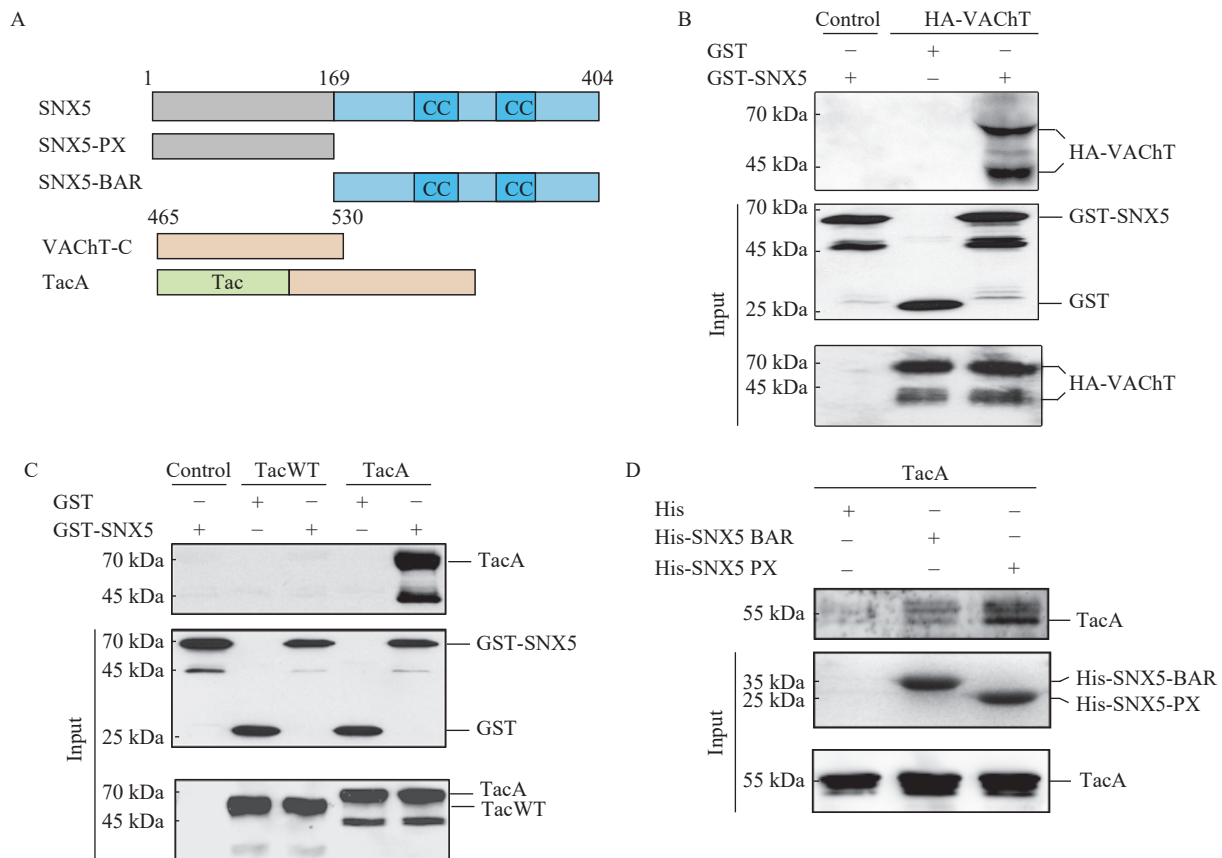


Fig. 3 Both PX and BAR domain of SNX5 interacted with the C-terminus of VACHT. A: Schematic diagram of VACHT and its deletion constructs. B: HA-VACHT was transiently transfected in COS7 cells for 48 hours, followed by cell lysates incubated with glutathione-sepharose immobilized GST-SNX5 and detected with anti-VACHT antibody by Western blotting. C: TacWT and TacA were transiently transfected in COS7 cells for 48 hours, followed by cell lysates incubated with glutathione-sepharose immobilized GST-SNX5 and analyzed with anti-IL2R α antibody by Western blotting. D: COS7 cells were transiently transfected with TacA for 48 hours. Cell lysates were incubated with Ni-NTA agarose immobilized His, His-SNX5-PX and His-SNX5-BAR recombinant proteins and detected with anti-IL2R α antibody by Western blotting. TacA: a chimeric protein fused VACHT C-terminus with an unrelated protein, Tac.

the stability of VACHT dramatically decreased by knocking down the expression of SNX5 using specific SNX5 siRNA (**Fig. 4A and B**). To identify whether the degradation of VACHT was mediated by lysosomal pathway, we treated HeLa cells with lysosomal inhibitor leupeptin or NH_4Cl in the presence of CHX. The result showed that both leupeptin and NH_4Cl rescued the degradation of VACHT (**Fig. 5A**). To confirm this result, we examined the distribution of VACHT in HeLa cells after treating with SNX5 siRNA with or without leupeptin using confocal microscopy. In control cells, VACHT was found to localize in some perinuclear areas, while in SNX5 siRNA cells, VACHT localized at the cell periphery rather than perinuclear areas. When blocking lysosomal proteolysis by leupeptin in SNX5-depleted cells, we observed most of VACHT

had accumulated in lysosomes (**Fig. 5B**).

Above all, these data suggested that SNX5 regulated the stability of VACHT and prevented the protein from degradation through lysosomal pathway.

Depleted SNX5 expression altered vesicular localization of VACHT in PC12 cells

We next investigated whether SNX5 executes its function on the SV targeting of VACHT. Using density gradient fractionation, we found that in stable PC12 expressing TacA cells, TacA localized primarily to the light fraction (lanes 9 to 12) of density sucrose gradients and colocalized preferentially with the SV marker synaptophysin, but not with the LDCVs marker Sg II (**Fig. 6A**). The result was consistent with our earlier research^[5]. In contrast, TacA in SNX5-depleted PC12 stable cells were found to localize not

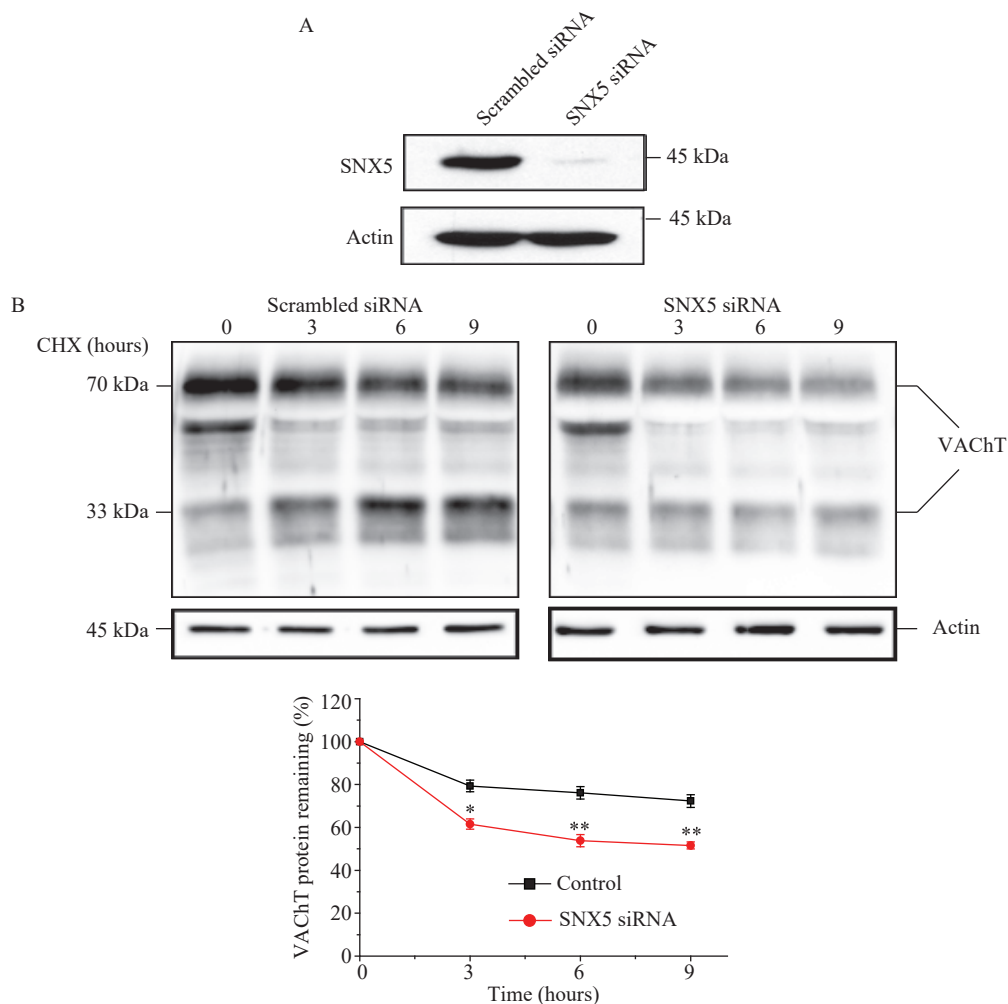


Fig. 4 Depletion of SNX5 induced the instability of VACHT. A: HeLa cells were transiently transfected with specific SNX5 siRNA or scrambled siRNA for 24 hours. SNX5 protein level in the cell lysates was detected with anti-SNX5 antibody by Western blotting. B: Half-life of VACHT expression was examined in control and SNX5-deleted HeLa cells after CHX (100 $\mu\text{g}/\text{mL}$) treatment at the indicated time points. VACHT expression level was detected with anti-VACHT antibody by Western blotting and quantified by densitometry analysis. The plots represent the mean of 3 independent experiments (* $P < 0.05$, ** $P < 0.01$; unpaired, two-tailed t -test, SNX5 siRNA vs. Control; error bars, standard error of the mean). CHX: cycloheximide.

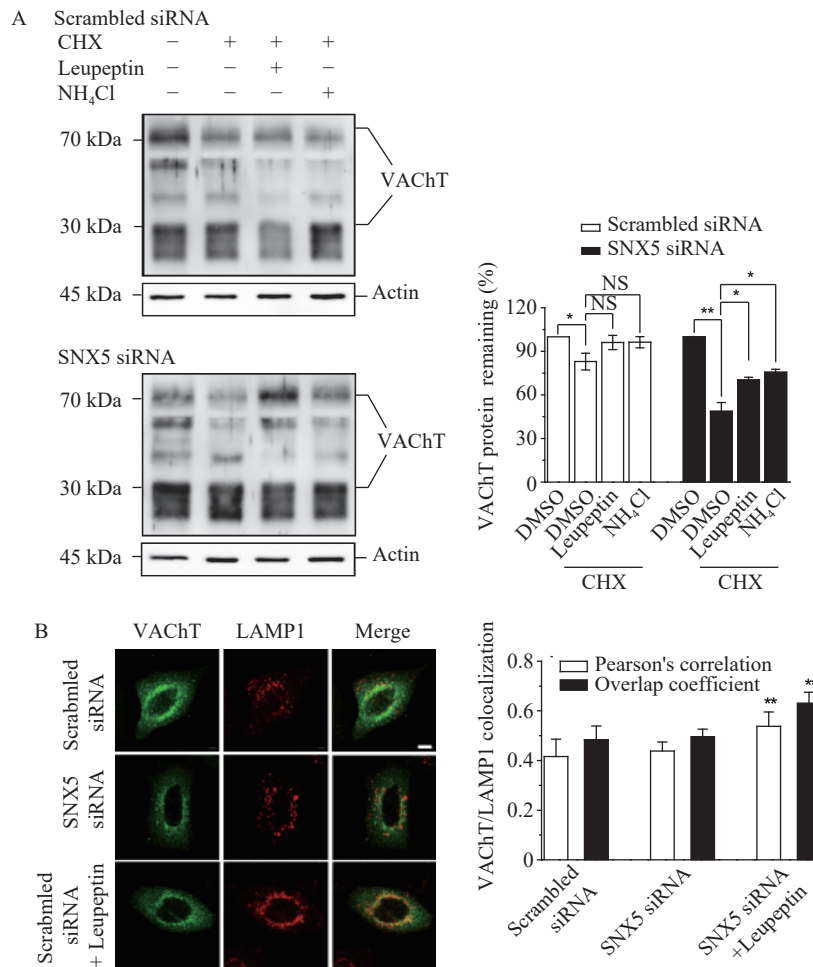


Fig. 5 Depletion of SNX5 led to lysosomal degradation of VACHT. A: VACHT expression was detected in control and SNX5-deleted HeLa cells followed by the treatment of CHX (100 μ g/mL) for 9 hours in the presence of DMSO (–), lysosomal inhibitors (100 μ g/mL leupeptin or 50 mmol/L NH₄Cl). VACHT expression level was detected with anti-VACHT antibody by Western blotting and quantified by densitometry analysis. The statistic data represent the mean of 3 independent experiments (* P <0.05, ** P <0.01; one-way ANOVA; error bars, standard error of the mean). B: Colocalization of VACHT with the lysosomal marker LAMP1 was examined by immunofluorescent staining in control and SNX5-depleted HeLa cells treated with CHX and leupeptin for 8 hours. The graph represented the mean of three independent experiments with 10 images each (n =3; ** P <0.01; unpaired, two-tailed t -test, SNX5 siRNA, SNX5 siRNA+Leupeptin vs. Scrambled siRNA; error bars, standard error of the mean). Scale bar, 10 μ m. CHX: cycloheximide.

only to SV fractions (lanes 5 to 8) but also to LDCV fractions (lanes 9 to 12) (**Fig. 6A**), indicating that SNX5 regulates the SV targeting of VACHT. Next, in order to investigate which domain of SNX5 determines this process, the subcellular distribution of TacA was examined in stable TacA cells transfected with full-length SNX5, SNX5-PX and SNX5-BAR. Like control cells expressing TacA only, cells co-transfected with TacA and SNX5 full-length showed one single peak in lanes 11 to 14, which indicated the distribution of SVs. In contrast, TacA cells expressed either SNX5-PX or SNX5-BAR showed a two-peak distribution (**Fig. 6B**), suggesting that TacA located in both SV and LDCV fraction. In addition, the statistical data showed that the percentage of TacA localized on SV was significantly reduced in cells transfected with SNX5 deletion mutants compared with control cells

and cells overexpressed wild type SNX5. To confirm whether SNX5 affects the distribution of VACHT on SVs, we used SNX5 specific siRNA to reduce the protein's endogenous expression and then examine colocalization between VACHT and synaptophysin in PC12 cells. As shown in **Fig. 6C**, compared with scrambled cell, the colocalization between VACHT and synaptophysin were significantly decreased.

Discussion

In this study, by using Y2H screen we identified SNX5 as a novel interaction partner of VACHT. Protein-protein interaction assays confirmed that SNX5 interacts physically and co-localized with VACHT. Functionally, SNX5 could stabilize the expression level of VACHT. Loss of SNX5 enhanced

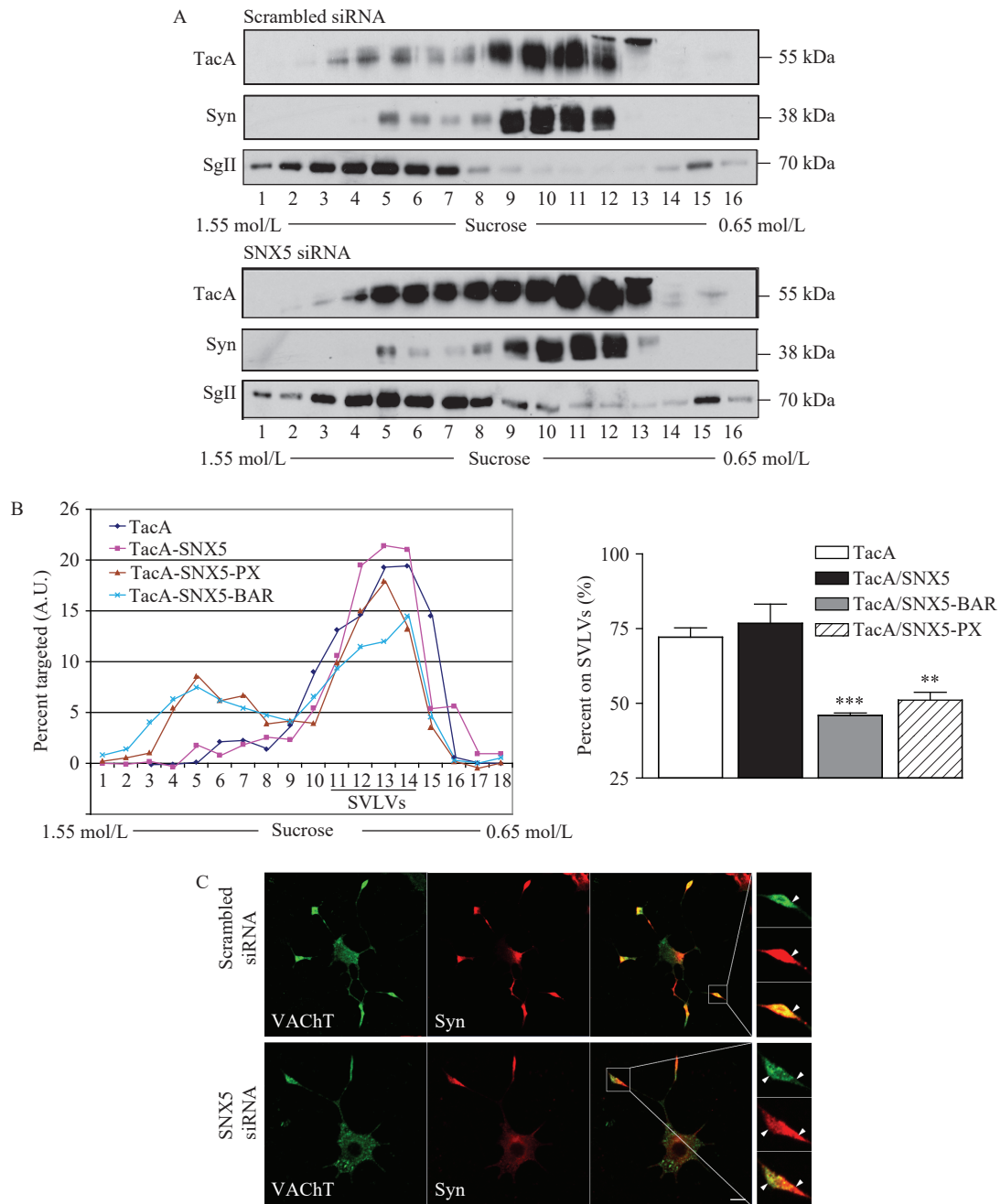


Fig. 6 Depleted SNX5 expression altered vesicular localization of VACHT in PC12 cells. **A:** Stable transformants of TacA PC12 cells were transfected with scrambled siRNA (upper panel) and SNX5 siRNA (lower panel) for 72 hours followed by homogenization and then fractionation through a density sucrose gradient (0.65 to 1.55 mol/L). Fractional association of TacA was profiled by comparison with markers for SVLVs and LDCVs with Western blotting. Synaptophysin, a marker of SVLVs; secretogranin II (Sg II), a marker of LDCVs. **B:** Stable transformants of TacA PC12 cells were transfected with wild type SNX5 and different mutants for 72 hours followed by homogenization and then fractionation through a density sucrose gradient (0.65 to 1.55 mol/L). The left graph represents the quantification of immunoreactivity for VACHT positive fractions. The right graph represents the percentage of SV-fractional association of VACHT in wild type SNX5 and deletion mutants transfected TacA cells compared with immunoreactivity of total fractional associated VACHT in TacA cells (based on three independent experiments, $**P < 0.01$, $***P < 0.001$; unpaired, two-tailed *t*-test, TacA/SNX5, TacA/SNX5-BAR, TacA/SNX5-PX vs. TacA; error bars, standard error of the mean). **C:** Stable transformants of VACHT PC12 cells were transfected with scrambled siRNA or SNX5 siRNA for 72 hours followed by examining the colocalization between VACHT and synaptophysin by immunofluorescent staining using specific antibodies. Scale bar, 10 μ m. TacA: a chimeric protein fused VACHT C-terminus with an unrelated protein, Tac; SVLVs: synaptic vesicle-like vesicles; LDCVs: large densecore vesicles.

the degradation of VACHT. Moreover, SNX5 could regulate trafficking and targeting of VACHT to SVs. Depletion of SNX5 significantly impaired the targeting of VACHT to SVs while increased its

targeting to LDCVs. On the basis of our findings we proposed a mechanistic role of SNX5 in regulating the stability of VACHT and facilitating the targeting of VACHT to SVs.

Previous work from our own group suggests that the signaling sequence within the C-terminus of VACHT is necessary and sufficient for its internalization and SV targeting^[5]. The endocytosis of VACHT seems to be mediated by clathrin-associated mechanism through the interaction of its C-terminal tail with AP2^[13]. Interestingly, in this study our approach of using TacA chimeric protein allows us to determine that the C-terminal domain of VACHT could also interact with SNX5. Since no direct interaction between AP3 and the C-terminus of VACHT has been detected^[6], our research first identifies a possible regulating machinery of the following intracellular events of VACHT after internalization. However, whether the interaction between the C-terminus of VACHT and SNX5 is dependent on the dileucine motif needs further research. Although the presence of negative charges upstream of the dileucine motif of VACHT does not seem to influence internalization of this transporter, it has been demonstrated that negative charges proximal to the dileucine motif can influence sorting to LDCVs in PC12 cells^[25]. VACHT contains a glutamic acid at position -4 and a serine in position-5 relative to the dileucine motif, which undergoes regulated phosphorylation by protein kinase C, enhancing VACHT targeting to LDCVs^[25]. In this paper we revealed that SNX5 could facilitate the SV targeting of VACHT. Depletion of SNX5 by SNX5 specific siRNA reduced VACHT targeting to SVs and enhanced the mistargeting of VACHT to LDCVs (**Fig. 6**). This result may provide a new mechanism of regulating VACHT sorting in SVs. Further studies are needed to investigate how SNX5 regulates VACHT sorting. For example, it is still unclear whether SNX5 regulate the VACHT sorting in cooperation with other components of the trafficking machinery. Although the interaction between SNX5 and VACHT may be retromer-independent, it is also possible for the retromer complex to contribute to regulating SNX5-mediated VACHT trafficking and sorting. The retromer complex has been shown to link with neurodegenerative diseases, like Alzheimer's disease and Parkinson's disease.

SNX5 is well-known as the key component of the retromer complex which mediates retrograde transport of membrane proteins from early endosomes to the TGN^[19,26]. Classical theories indicated that the cargo recognition complex (CRC) which is made up of Vps26/29/35 is responsible for the recognition and binding of cargo proteins^[27–28], while SNX proteins in the mammalian retromer complex including SNX1/2 and SNX5/6 are exclusively responsible for membrane remodeling in order to form a tubule-shaped extension^[29–31]. Interestingly, recent studies from two

separate research groups suggested that it is SNX-BAR proteins but not CSC mediating cargo recognition^[32–33]. Moreover some other papers showed that SNX5 could interact with cargo proteins, acting in a retromer-independent role. Previous studies have identified the D1 dopamine receptor (D1R) as a binding partner of SNX5^[34–35]. The research demonstrated that SNX5 and D1R basally interact at the plasma membrane and after D1R internalization the two proteins continue interaction in the cytoplasm. In addition, SNX5 also interacts with G-protein-coupled receptor kinase 4 (GRK4)^[34]. These results suggested that SNX5 could act in a retromer-independent role. Here we reported that the interaction between SNX5 and VACHT was mediated by its both BAR and PX domains (**Fig. 2**). The BAR domains in SNXs are known to mediate dimerization and membrane curvature^[19,31], while the PX domains in SNX5 contain a sequence that binds to PI(4,5)P₂^[36]. Studies have almost exclusively focused on the given abilities of these two important domains, but there is accumulating evidence that both BAR and PX domains can also act as protein-interaction partners. A latest research revealed that SNX9 interacts with podocin through the BAR domain of SNX9^[37]. And the PX domains of a number of SNXs, including SNX1, 2, 4, and 6 could associate with the cytoplasmic tails of transforming growth factor β receptor family members^[38].

In summary, we have identified SNX5 as a novel binding partner of VACHT. Depletion of SNX5 resulted in VACHT lysosomal degradation and mistargeting of VACHT to LDCVs. Thus, SNX5 regulates the stability of VACHT and mediates the correct targeting of VACHT to SVs.

Acknowledgments

This work was supported by the National Natural Science Foundation of China (No. 31371436 and No. 8157051134) and by the laboratory start-up grant from Nanjing Medical University to YL. The funders had no role in study design, data collection and analysis, decision to publish, or preparation of the manuscript.

References

- [1] Roghani A, Feldman J, Kohan SA, et al. Molecular cloning of a putative vesicular transporter for acetylcholine[J]. *Proc Natl Acad Sci, U S A*, 1994, 91(22): 10620–10624.
- [2] Song HJ, Ming GL, Fon E, et al. Expression of a putative vesicular acetylcholine transporter facilitates quantal transmitter packaging[J]. *Neuron*, 1997, 18(5): 815–826.
- [3] Liu YJ, Krantz DE, Waites C, et al. Membrane trafficking of neurotransmitter transporters in the regulation of synaptic

- transmission[J]. *Trends Cell Biol*, 1999, 9(9): 356–363.
- [4] Tan PK, Waites C, Liu YJ, et al. A leucine-based motif mediates the endocytosis of vesicular monoamine and acetylcholine transporters[J]. *J Biol Chem*, 1998, 273(28): 17351–17360.
- [5] Colgan L, Liu H, Huang SY, et al. Dileucine motif is sufficient for internalization and synaptic vesicle targeting of vesicular acetylcholine transporter[J]. *Traffic*, 2007, 8(5): 512–522.
- [6] Barbosa Jr J, Ferreira LT, Martins-Silva C, et al. Trafficking of the vesicular acetylcholine transporter in SN56 cells: a dynamin-sensitive step and interaction with the AP-2 adaptor complex[J]. *J Neurochem*, 2002, 82(5): 1221–1228.
- [7] Voglmaier SM, Kam K, Yang H, et al. Distinct endocytic pathways control the rate and extent of synaptic vesicle protein recycling[J]. *Neuron*, 2006, 51(1): 71–84.
- [8] Saheki Y, De Camilli P. Synaptic vesicle endocytosis[J]. *Cold Spring Harb Perspect Biol*, 2012, 4(9): a005645.
- [9] Kwon SE, Chapman ER. Glycosylation is dispensable for sorting of synaptotagmin 1 but is critical for targeting of SV2 and synaptophysin to recycling synaptic vesicles[J]. *J Biol Chem*, 2012, 287(42): 35658–35668.
- [10] Nakata T, Terada S, Hirokawa N. Visualization of the dynamics of synaptic vesicle and plasma membrane proteins in living axons[J]. *J Cell Biol*, 1998, 140(3): 659–674.
- [11] Stewart RS, Teng HB, Wilkinson RS. "Late" macroendosomes and acidic endosomes in vertebrate motor nerve terminals[J]. *J Comp Neurol*, 2012, 520(18): 4275–4293.
- [12] Kim JY, Choi BK, Choi MG, et al. Solution single-vesicle assay reveals PIP₂-mediated sequential actions of synaptotagmin-1 on SNAREs[J]. *EMBO J*, 2012, 31(9): 2144–2155.
- [13] Kim MH, Hersh LB. The vesicular acetylcholine transporter interacts with clathrin-associated adaptor complexes AP-1 and AP-2[J]. *J Biol Chem*, 2004, 279(13): 12580–12587.
- [14] Haberman A, Williamson WR, Epstein D, et al. The synaptic vesicle SNARE neuronal Synaptobrevin promotes endolysosomal degradation and prevents neurodegeneration[J]. *J Cell Biol*, 2012, 196(2): 261–276.
- [15] Fewou SN, Plomp JJ, Willison HJ. The pre-synaptic motor nerve terminal as a site for antibody-mediated neurotoxicity in autoimmune neuropathies and synaptopathies[J]. *J Anat*, 2014, 224(1): 36–44.
- [16] Koo SJ, Markovic S, Puchkov D, et al. SNARE motif-mediated sorting of synaptobrevin by the endocytic adaptors clathrin assembly lymphoid myeloid leukemia (CALM) and AP180 at synapses[J]. *Proc Natl Acad Sci U S A*, 2011, 108(33): 13540–13545.
- [17] Goh GY, Huang H, Ullman J, et al. Presynaptic regulation of quantal size: K⁺/H⁺ exchange stimulates vesicular glutamate transport[J]. *Nat Neurosci*, 2011, 14(10): 1285–1292.
- [18] Liu H, Liu ZQ, Chen CXQ, et al. Inhibitory regulation of EGF receptor degradation by sorting nexin 5[J]. *Biochem Biophys Res Commun*, 2006, 342(2): 537–546.
- [19] Bonifacino JS, Hurlley JH. Retromer[J]. *Curr Opin Cell Biol*, 2008, 20(4): 427–436.
- [20] Seet LF, Hong WJ. The Phox (PX) domain proteins and membrane traffic[J]. *Biochim Biophys Acta (BBA) - Mol Cell Biol Lipids*, 2006, 1761(8): 878–896.
- [21] Takamori S, Holt M, Stenius K, et al. Molecular anatomy of a trafficking organelle[J]. *Cell*, 2006, 127(4): 831–846.
- [22] Jung N, Wienisch M, Gu MY, et al. Molecular basis of synaptic vesicle cargo recognition by the endocytic sorting adaptor stonin 2[J]. *J Cell Biol*, 2007, 179(7): 1497–1510.
- [23] Palfrey HC, Artalejo CR. Vesicle recycling revisited: rapid endocytosis may be the first step[J]. *Neuroscience*, 1998, 83(4): 969–989.
- [24] Svingos AL, Colago EEO, Pickel VM. Vesicular acetylcholine transporter in the rat nucleus accumbens shell: subcellular distribution and association with μ -opioid receptors[J]. *Synapse*, 2001, 40(3): 184–192.
- [25] Krantz DE, Waites C, Oorschot V, et al. A phosphorylation site regulates sorting of the vesicular acetylcholine transporter to dense core vesicles[J]. *J Cell Biol*, 2000, 149(2): 379–396.
- [26] Seaman MNJ. Cargo-selective endosomal sorting for retrieval to the Golgi requires retromer[J]. *J Cell Biol*, 2004, 165(1): 111–122.
- [27] McGough IJ, Cullen PJ. Recent advances in retromer biology[J]. *Traffic*, 2011, 12(8): 963–971.
- [28] Seaman MNJ. The retromer complex - endosomal protein recycling and beyond[J]. *J Cell Sci*, 2012, 125(20): 4693–4702.
- [29] Griffin CT, Trejo J, Magnuson T. Genetic evidence for a mammalian retromer complex containing sorting nexins 1 and 2[J]. *Proc Natl Acad Sci U S A*, 2005, 102(42): 15173–15177.
- [30] Oosawa H, Fujii T, Kawashima K. Nerve growth factor increases the synthesis and release of acetylcholine and the expression of vesicular acetylcholine transporter in primary cultured rat embryonic septal cells[J]. *J Neurosci Res*, 1999, 57(3): 381–387.
- [31] Hall DD, Dai SP, Tseng PY, et al. Competition between α -actinin and Ca²⁺-calmodulin controls surface retention of the L-type Ca²⁺ channel Ca_v1.2[J]. *Neuron*, 2013, 78(3): 483–497.
- [32] Wang W, Bouhours M, Gracheva EO, et al. ITSN-1 controls vesicle recycling at the neuromuscular junction and functions in parallel with DAB-1[J]. *Traffic*, 2008, 9(5): 742–754.
- [33] Mohrmann R, Matthies HJ, Woodruff III E, et al. Stoned B mediates sorting of integral synaptic vesicle proteins[J]. *Neuroscience*, 2008, 153(4): 1048–1063.
- [34] De Rubeis S, Pasciuto E, Li KW, et al. CYFIP1 coordinates mRNA translation and cytoskeleton remodeling to ensure proper dendritic spine formation[J]. *Neuron*, 2013, 79(6): 1169–1182.
- [35] Poon WW, Carlos AJ, Aguilar BL, et al. β -Amyloid (A β) oligomers impair brain-derived neurotrophic factor retrograde trafficking by down-regulating ubiquitin C-terminal hydrolase, UCH-L1[J]. *J Biol Chem*, 2013, 288(23): 16937–16948.
- [36] Palaniyappan L, Simmonite M, White TP, et al. Neural primacy of the salience processing system in schizophrenia[J]. *Neuron*, 2013, 79(4): 814–828.
- [37] Boassa D, Berlanga ML, Yang MA, et al. Mapping the subcellular distribution of α -synuclein in neurons using genetically encoded probes for correlated light and electron microscopy: implications for Parkinson's disease pathogenesis[J]. *J Neurosci*, 2013, 33(6): 2605–2615.
- [38] Parks WT, Frank DB, Huff C, et al. Sorting nexin 6, a novel SNX, interacts with the transforming growth factor- β family of receptor serine-threonine kinases[J]. *J Biol Chem*, 2001, 276(22): 19332–19339.